Applicability of ferric(III) hydroxide as a phosphate-selective adsorbent for sewage treatment

Choon-Ki Na, Ga-Yeon Park and Hyun Ju Park

ABSTRACT

This research was undertaken to evaluate the usability of ferric(III) hydroxide for phosphate removal from sewage. Batch adsorption experiments, partly fixed bed column experiments, were conducted to study the influence of various factors, competing anions and contact time on the adsorption of phosphate on ferric(III) hydroxide. Processing ferric iron in the form of akaganeite (β-FeOOH) greatly increased the adsorption capacity for phosphate. The optimum phosphate removal was observed in the $pH_{eq} \leq 6.0$. All results from this study demonstrate the potential usability of β-FeOOH as a good phosphate-selective adsorbent for the phosphate removal system for a sewage treatment plant.

Key words | adsorption selectivity, akaganeite, isotherm, kinetics, phosphate removal, sewage treatment

Choon-Ki Na
Ga-Yeon Park
Department of Environmental Engineering,
Mokpo National University,
Jeonnam 58554,
South Korea

Hyun Ju Park (corresponding author)
Institute of Engineering,
Seoul National University,
1 Gwanak-ro, Gwanak-gu, 08826, Seoul,
Republic of Korea
E-mail: *narjjis@hanmail.net*

HIGHLIGHTS

- Recovery of phosphate from sewage and wastewater to control eutrophication.
- To develop phosphate-selective absorbents.
- The potential usability of β-FeOOH as phosphate-selective adsorbent.
- β-FeOOH can be applied for the phosphate removal system.
- The phosphate adsorption capacity was increased to β-FeOOH>PA rein>Fe(OH)3.

INTRODUCTION

Phosphorus together with nitrogen is an essential nutrient in aquatic ecosystems as well as agriculture. However, excessive input of phosphate in water bodies usually triggers eutrophication, which threatens the aquatic ecosystem (Genkai-Kato & Carpenter 2005; Conley *et al.* 2009; Lewis *et al.* 2011). Thus, methods of sewage treatment focus on the efficiency improvement of phosphorus compound reduction (Schindler *et al.* 2016). In Korea, the discharge limits of T-P in sewage treatment plants has been greatly strengthened from 2.0 mg/L to 0.2 mg/L, to prevent eutrophication. China has also strengthened the maximum P allowed for secondary effluents from wastewater treatment plants from 1.0 mg/L to 0.5 mg/L (Wu *et al.* 2019). As discharge limits of nutrients become more stringent, the demands for an introduction of advanced treatment techniques continue to increase in sewage treatment for the appropriate removal of phosphorus and nitrogen. Various advanced treatment techniques, as the form of a hybrid process integrated into existing biological treatment process, including chemical precipitation, biological phosphorus removal, and adsorption, etc., have been developed for removal of phosphate from sewage and wastewater to control eutrophication (Gogate & Pandit 2004; Park & Na 2009; Park *et al.* 2016; Zhao *et al.* 2016; Omwene *et al.* 2018; Jiang *et al.* 2019).

In recent years, chemical phosphate removal facilities have been widely adopted as advanced treatment processes for sewage due to their relatively simple treatment process, manageable and high reliability of treatment efficiency,

doi: 10.2166/wst.2021.180

although their chemical and waste disposal costs are very high. However, chemical and biological methods commonly used for phosphorus removal are not economically and cost-effective in small treatment plants (Gajewska *et al.* 2011). Moreover, although it is well demonstrated that the application of commercial coagulants such as polyaluminum chloride (PAC) is very effective in removing phosphate from sewage, and the presence of aluminum is essential to plants growth, but excess can be toxic to humans as well as plants (Kochian & Jones 1997). It is known that potable water highly contaminated with aluminum (320 mg/L) can affect the digestive system, and cause skin rashes and memory loss (Kasprzyk & Gajewska 2019). The impact of aluminum on Parkinson and Alzheimer disease is also the subject of many research studies (Bondy 2014). Thus, these facts suggest that another efficient technology needs to be found.

Together with chemical precipitation method, it is well known that adsorption is a promising method to remove phosphate due to its advantages of operational simplicity, environmental friendliness, and higher effectiveness even at low phosphate concentrations (Méndez-Álvarez *et al.* 2002). Accordingly, many adsorbents, such as zeolite, activated carbon, industrial solid wastes such as red mud, fly ash, and slag, ion-exchange resin, and polymeric materials have been investigated for phosphate removal (Sendrowski & Boyer 2013; Park *et al.* 2015; Wang *et al.* 2016). Recently, metal-based adsorbents have been extensively investigated to selectively adsorb phosphate anions in wastewater, such as magnesium oxide-enriched biochar, iron-modified biochars, hydrous zirconia-modified zeolite, hydroxy-iron-aluminum pillared bentonite, and lanthanum-modified diatomite (Yan *et al.* 2010; Zhang *et al.* 2012; Fan *et al.* 2017; Yang *et al.* 2018; Wu *et al.* 2019). Most of these adsorbents exhibit high adsorption capacity and selectivity for phosphate. However, there is a growing demand for more efficient, cost-effective and effective regenerative adsorbents.

It is known that the specific adsorption of phosphate with iron oxyhydroxides is important in controlling phosphate in industrial and engineering processes, as well as in the environment (Krom & Berner 1980). Iron oxyhydroxide is known to occur commonly as goethite (α-FeOOH), akaganeite (β-FeOOH), and lepidocrocite (γ-FeOOH). Among them, goethite is the most widespread iron oxide in the natural environment and has been used in various adsorption studies for phosphate, fluoride, arsenate, selenite and etc. Conversely, akaganeite is a rare mineral in nature, and has semiconductor, catalytic, and ion-exchange properties (Villalba *et al.* 2010).

The aim of this study was to develop phosphate-selective absorbents that are not affected by co-existence anions, especially sulfuric acid and chlorine ions, to apply the adsorption process as a phosphate removal facility in urban sewage treatment plants. The phosphate adsorption and adsorption selectivity of akaganeite (β-FeOOH) were evaluated by a batch-type adsorption experiment and a fixed bed column experiment. The akaganeite was processed into a spherical bead-type adsorbent combined with a polymer material and used in the adsorption experiments. The experiments were conducted with synthetic pure phosphate solutions and with discharge water from a public sewage treatment plant.

EXPERIMENTAL

Materials and reagents

Ferric chloride anhydrous ($FeCl_3$, 97%) was used as source of Fe(III) to prepare iron (oxy)hydroxide adsorbent. NaOH (98%) was used to precipitate akaganeite (β-FeOOH) from the $FeCl_3$ solution. Polyacrylonitrile (PAN, MW = 150,000) as a binder, polyvinyl alcohol (PVA, MW = 500) as a porosity controller, and dimethyl sulfoxide (DMSO) as a solvent were used to make akaganeite powder into a spherical bead. The discharge water was collected from a sewage treatment plant located in Mokpo city, Korea and filtered through a GF-C filter paper and then used as a real wastewater for adsorption experiments. The discharge water used in experiments had a pH of 6.8, 15.1 mg/L nitrate, 3.4 mg/L phosphate, 442 mg/L chloride and 69 mg/L sulfate ions.

Extra pure chemicals, NaH_2PO_4, Na_2SO_4, and NaCl were used to prepare anion solution for sorption experiments. The working solutions were prepared by dissolving the chemicals in deionized water (DIW) or in a pH buffer solution. The pH buffer solution was composed of CH_3COOH and CH_3COONa, with a total acetate concentration of 0.01 M (pH 4.7). Commercial anion-exchange resin, PA308 resin ($-N^+(CH_3)_3Cl^-$, Samyang Co.) was used as a comparative adsorbent.

Preparation of adsorbent

Akaganeite (β-FeOOH) was synthesized using a procedure reported previously (Chitrakar *et al.* 2006). First, 0.1 M NaOH solution was slowly added to a 0.1 M $FeCl_3$ solution at room temperature until the pH of the mixture was attained around 10, the mixture was stirred mechanically

during the addition of the NaOH solution. The suspension was further stirred for 12 h. The precipitate was separated by centrifugation, washed with DIW until neutral, and finally dried in air at room temperature. Dried precipitate was pulverized with a particle size range of 150–200 mesh and then used as an adsorption functional inorganic powder to prepare a spherical bead-type adsorbent combined with polymeric materials. The spherical bead-type adsorbent was prepared as follows: 0.3 g of PAN and 0.1 g of PVA were dissolved in 6 mL DMSO solvent, and then 2 g of akaganeite powders was added to this solution with continuously mixing to obtain homogeneous composite solution. The composite solution was dropped into DIW stirring at 120 rpm and room temperature by using a syringe with an air spray. The suspension was further stirred for more than 12 h to dissolve the PVA component in the spherical beads. The solidified beads were separated and washed with DIW, and air dried for more than 24 h at room temperature, and then dried completely at 60 °C to remove the solvent. The spherical beads used as an adsorbent have a grain size range of 10–20 mesh.

Adsorption experiments

The adsorbent properties of ferrous compounds were evaluated based on a batch test, in which 0.1 g of adsorbent was added to high-density polyethylene (HDPE) bottles containing 100 mL of phosphate solution of known concentrations. The bottles were settled in an incubator shaker and then continuously shaken at 25 °C and 120 rpm for a predetermined time period. After the predetermined sorption time, solid and liquid phases were separated using GF-C filter, phosphate anion concentrations in the liquid phase were measured. The initial (C_0) and equilibrium (C) phosphate anion concentrations were determined by UV spectrometer (Shimadzu UV-2401PC, Japan). The adsorbent-phase phosphate anion concentration, q(mg/g) was calculated from the anion mass balance using the following formula:

$$q = \frac{V(C_0 - C)}{W} \quad (1)$$

where V is the volume of solution(L) and W is the weight of dry adsorbent(g).

The effect of different pH values on phosphate adsorption was studied by adjusting the pH of solution using either 0.1 M HCl or 0.1 M NaOH solutions to the required pH range of 3–12 after the adsorption equilibrium.

The effect of competing anions such as Cl^- and SO_4^{2-} ion co-existing in the sewage with phosphate ion on the phosphate adsorption onto adsorbent was evaluated based on the binary system by referring to the chemical composition of discharge water from sewage treatment plant.

To evaluate the regeneration efficiency of adsorbent, repeated adsorption–regeneration experiments were conducted using an alkaline washing process, where phosphate-sorbed adsorbent was immersed in 0.1 N NaOH solution and shaken for 1 h at room temperature. After complete desorption, the adsorbent was washed with DIW until the pH was neutral and dried at 60 °C. The adsorption–regeneration cycle was repeated 10 times and the phosphate adsorption capacity was measured for each cycle.

RESULTS AND DISCUSSION

Characteristics of adsorbent

SEM image (Figure 1(a)) and XRD pattern (Figure 1(b)) of β-FeOOH, and morphology (Figure 1(a)) of cross-section of β-FeOOH/PAN bead are shown. The XRD pattern indicates that the β-FeOOH used in this study was a two-line amorphous akaganeite with poor crystallinity, which is consistent with previous studies (Fu *et al.* 2018; Zhang *et al.* 2019). The point of zero charge (PZC) of β-FeOOH estimated from zeta potential measurements (Otsuka ELS-Z1, Japan) at different pHs is about 8.0, similar to the results reported by other studies (Chitrakar *et al.* 2006). The BET specific surface area and pore volume of the β-FeOOH measured by a surface area and porosity analyzer (Micrometrics ASAP2010, USA) are 173.5 m^2/g and 0.38 cm^3/g, respectively, suggested that the β-FeOOH can be used as a good adsorbent for phosphate.

Figure 2 shows the phosphate adsorption capacity of ferric hydroxide ($Fe(OH)_3$, 90%), akaganeite (β-FeOOH) and commercial anion-exchange resin (PA308), based on the adsorption amount obtained by a batch mode adsorption test, in which 0.1 g of each adsorbent is added to 100 mL of 1 mM NaH_2PO_4 solution and stirred at 25 °C for 12 hours. The phosphate adsorption capacity was increased to β-FeOOH > PA308 > $Fe(OH)_3$. This indicates that, when processing Fe^{3+} in the form of β-FeOOH, the adsorption capacity for phosphate ion was higher than that of a commercial anion-exchange resin as well as ferric hydroxide.

Also shown in Figure 2, the difference in adsorption capacity between the composite bead and the powder was about 15%. This can be explained by the effect of the PAN content used as binder in the composite beads, which

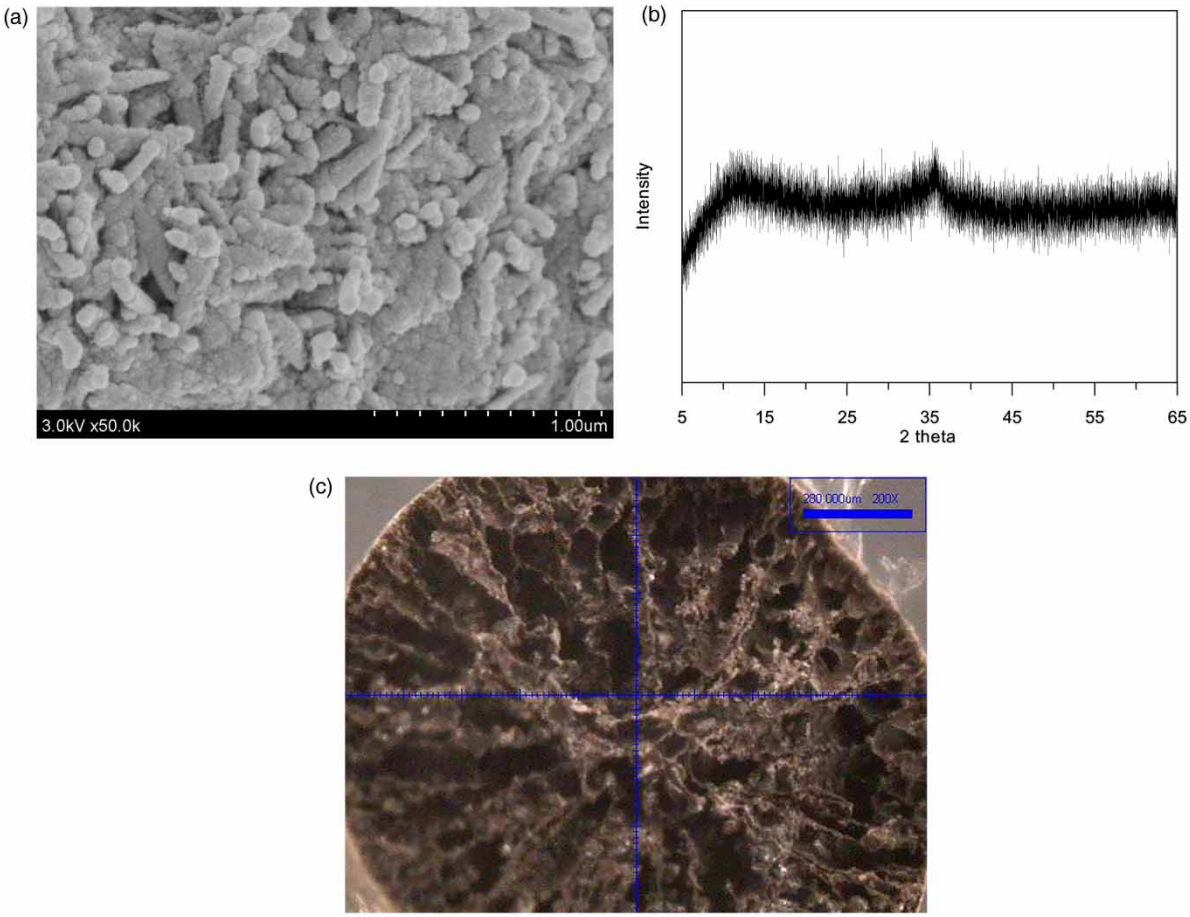

Figure 1 | SEM image (a) and XRD pattern (b) of β-FeOOH, and morphology (c) of cross-section of β-FeOOH/PAN bead.

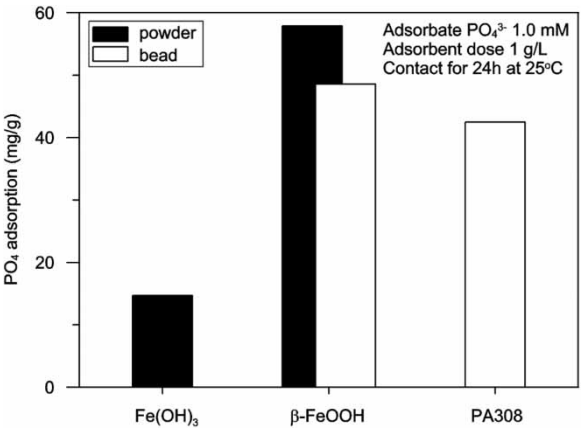

Figure 2 | PO_4-P adsorption on $Fe(OH)_3$, β-FeOOH and commercial PA308 resin.

means that the adsorption capacity of the inorganic adsorbent has not been seriously decreased in the process of manufacturing the powder into spherical composite beads.

Effect of pH

The pH of a solution is an important parameter in the adsorption process because the speciation of anions and the surface characteristics of the adsorbent are influenced by the pH value. To study the effect of solution pH on phosphate adsorption by β-FeOOH, the experiment was conducted with 0.5 mM NaH_2PO_4 solution at different pH values (2.5–12.0). Figure 3 shows the results of the phosphate adsorption on β-FeOOH as a function of the equilibrium pH of solution. The phosphate adsorption on the β-FeOOH remained almost constant until the pH of the solution was increased up to around 6, and then sharply decreased with increase in pH. Similar findings have been observed in the phosphate adsorption by other metal-based adsorbents (Yan *et al.* 2010; Fu *et al.* 2018). The removal of phosphate from the solution by β-FeOOH was nearly 100% at pH < 6. A possible explanation for the high adsorption capacity of β-FeOOH at pH < 6 is the comprehensive effect of the formation of

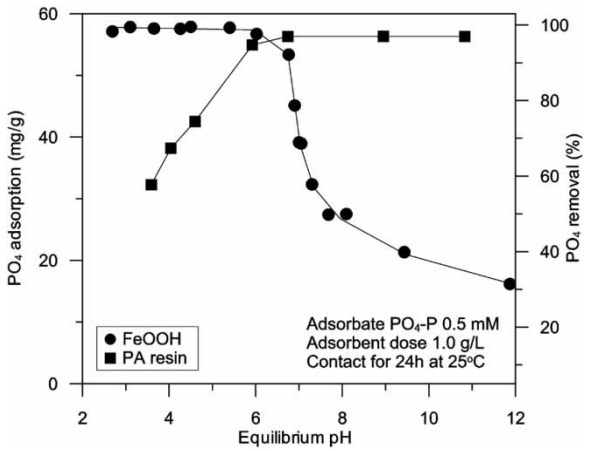

Figure 3 | Effect of pH on PO_4-P adsorption onto β-FeOOH. Also shown onto anion-exchange polyamide (PA) resin.

outer-sphere complexes by electrostatic force and inner-sphere complexes by ligand exchange. The decrease of adsorption capacity in alkaline region may be interpreted by change in adsorbent surface charge rather than by ion competition. As the pH of solution was increased, the number of positively charged surface sites decreased, which is unfavorable to the sorption of negatively charged anions. The point of zero charge (pzc) of β-FeOOH is determined at about pH 8. When pH approached pH_{pzc}, the positively charged surface sites, which served as phosphate-binding sites, significantly decreased with the increase in pH. The pH effect on phosphate adsorption of conventional anion-exchange resin (PA308) was different from that of β-FeOOH, as shown in Figure 3. The phosphate adsorption capacity of the anion-exchange resin tends to increase continuously with increasing pH of solution up to 7, and then maintained constant values. At pH > 7, the phosphate ion was almost removed (≥95%) from the solution by adsorption of the anion-exchange resin, which indicates probably that it was affected by changes in ionic specification of phosphate. As the pH increases, the phosphates such as $H_2PO_4^-$, HPO_4^{2-}, and PO_4^{3-} become the major species, which are more favorable to adsorption by anion-exchange resin, but not by β-FeOOH due to greater electrostatic repulsion between the more negatively charged surfaces and phosphate anions.

Adsorption isotherms

In order to study the adsorption isotherm of the β-FeOOH for phosphate, the β-FeOOH of 0.1 g comes into contact with the phosphate solution of 100 mL at concentrations in the range of 0.2–1.0 mmol/L. The phosphate solutions were prepared using the acetic acid buffer solution (pH 4.7), to minimize the effects of pH on the adsorption capacity of β-FeOOH. Each sample was allowed to equilibrate for 24 h at 25 °C, with constant shaking at 120 rpm, prior to analysis for the final phosphate ion concentration. The experimental data obtained were plotted in a linearised form of Langmuir (Langmuir 1918) and Freundlich isotherm (Freundlich 1906) models as shown below:

$$\frac{C_e}{q_e} = \frac{1}{bq_m} + \frac{C_e}{q_m} \quad (2)$$

$$\ln q_e = \ln K_F + \frac{1}{n} \ln C_e \quad (3)$$

where C_e is the equilibrium concentration (mg/L), q_e is the amount adsorbed at equilibrium (mg/g), q_m is the Langmuir constants related to the maximum monolayer adsorption capacity (mg/g), b is the Langmuir constants related to the energy of adsorption (L/mg), K_F and n are the Freundlich constants related to the sorption capacity of the adsorbent and the magnitude of the adsorption driving force, respectively. Figure 4 shows the experimental data and isotherm models for the adsorption of phosphate ion on β-FeOOH. The adsorption parameters determined by using the isotherm equations are summarized in Table 1. The linear fit of the experimental data to the Langmuir model exhibited a correlation coefficient of 0.9986, and the maximum

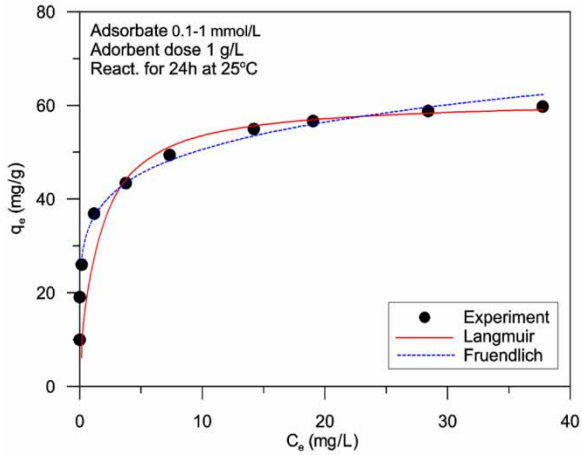

Figure 4 | Adsorption isotherms for PO_4-P on β-FeOOH.

Table 1 | Langmuir and Freundlich isotherm parameters

Langmuir isotherm			Freundlich isotherm		
q_m(mg/g)	b(L/mg)	R^2	K_F(mg/g)(L/mg)$^{1/n}$	n	R^2
60.98	0.896	0.9986	35.35	6.398	0.9926

adsorption capacity and b were found to be 60.98 mg/g and 0.896 L/mg, respectively. Conversely, the correlation coefficient for the fitting of the experimental data to the Freundlich model were found to be 0.9926. The K_F value and the n value were determined to be 35.35 (mg/g) (L/mg) 1/n and 6.398, respectively. The magnitudes of n value were in the level of good ($n \geq 2$) favorability of adsorption. A comparison of the correlation coefficients for the fit of the experimental data to the two isotherm models revealed that the Langmuir isotherm model provided the best fit; this indicated the predominance of monolayer adsorption.

The phosphate adsorption capacities of various adsorbents reported in the literature are summarized in Table 2.

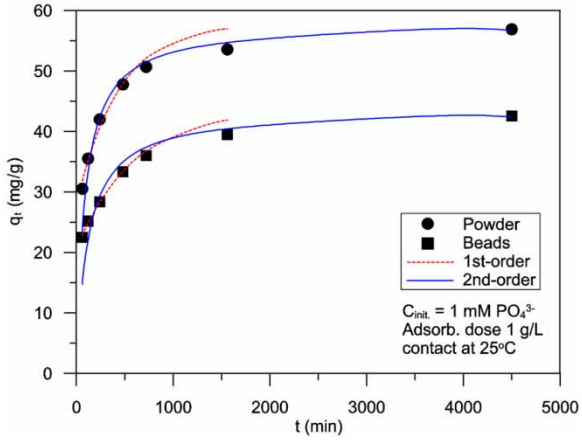

Figure 5 | Adsorption rates of PO_4-P on β-FeOOH.

Adsorption kinetics

The kinetics of the phosphate adsorption on β-FeOOH was studied, and the results are presented in Figure 5. The experimental data were fitted with the pseudo-first-order (Lagergren 1898) and pseudo-second-order (Ho & McKay 1998) kinetic models, as shown below:

$$\ln\,(q_e - q_t) = \ln q_e - k_1\, t \tag{4}$$

$$\frac{t}{q_t} = \frac{1}{k_2\, q_e^2} + \frac{t}{q_e} \tag{5}$$

where q_e and q_t are the amount of adsorbate adsorbed at equilibrium and time t (mg/g), and k_1 and k_2 are the rate constants of pseudo-first-order adsorption (min – 1) and of pseudo-second-order adsorption (g/mg min), respectively. The rate constants (k_1 and k_2) determined by using the kinetic models are summarized in Table 3. From the values in the table, we concluded that the pseudo-second-order kinetic equation represented the adsorption process better than the pseudo-first-order kinetics equation, regardless of the form of adsorbent. The fact that the phosphate adsorption on β-FeOOH follows the second-order type reaction, indicates that in the adsorption process, concentrations of both adsorbate and adsorbent are involved in rate-determining steps, which may be a chemical sorption or chemisorption (Ho & McKay 1998). It is known that the ordinary type of exchange processes is more rapid and controlled mainly by diffusion, whereas those in the chelating exchanger are slower and controlled either by particle diffusion mechanisms or by a second-order chemical reaction (Kantipuly *et al.* 1990).

Effect of competitive anions

One of the major problems which limit the wide application of adsorption method to eliminate pollutants is the ion selectivity for an adsorbent. Figure 6 shows the effects of

Table 2 | Comparison of phosphate adsorption capacity for various adsorbents

Adsorbent	q_m (mg P/g)	Experimental conditions	Reference
Activated aluminum oxide	12.0–13.8	pH 5.5, 8.2 C_0 4 mg/L	Genz *et al.* (2004)
Granulated ferric hydroxide	16.9–23.3	pH 5.5, 8.2 C_0 4 mg/L	Genz *et al.* (2004)
Al-bentonite	12.7	pH 3.0, C_0 25–60 mg/L	Yan *et al.* (2010)
Ca-rich sepiolite	32.0	pH 4.8, C_0 5–1,000 mg/L	Yin *et al.* (2011)
La-bentonite	14.4	pH 7.1 C_0 200 mg/L	Kurzbaum & Bar Shalom (2016)
Goethite	16.5	pH 7.0 C_0 65–326 mg/L	Ajmal *et al.* (2018)
Mag@Fh-La	44.8	pH 6.28, C_0 2–120 mg/L	Fu *et al.* (2018)
Feroxyhyte	18.2	pH 3.0 C_0 4–40 mg/L	Li *et al.* (2019)
La-diatomite	58.7	pH 5.6, C_0 10–100 mg/L	Wu *et al.* (2019)
Akaganeite	19.9	pH 4.7, C_0 0.1–1.0 M	This study

Table 3 | First- and second-order kinetic parameters

Form	Experiment q_e(mg/g)	Pseudo-first-order kinetics[a] k_1(min^{-1})	q_e(mg/g)	R^2	Pseudo-second-order kinetics k_2(g/mg min)	q_e(mg/g)	R^2
Powder	56.90	2.0×10^{-3}	28.13	0.9782	1.96×10^{-4}	57.80	0.9998
Beads	42.56	1.6×10^{-3}	22.28	0.9946	1.97×10^{-4}	43.48	0.9994

[a]Only for initial adsorption period (0–720 min).

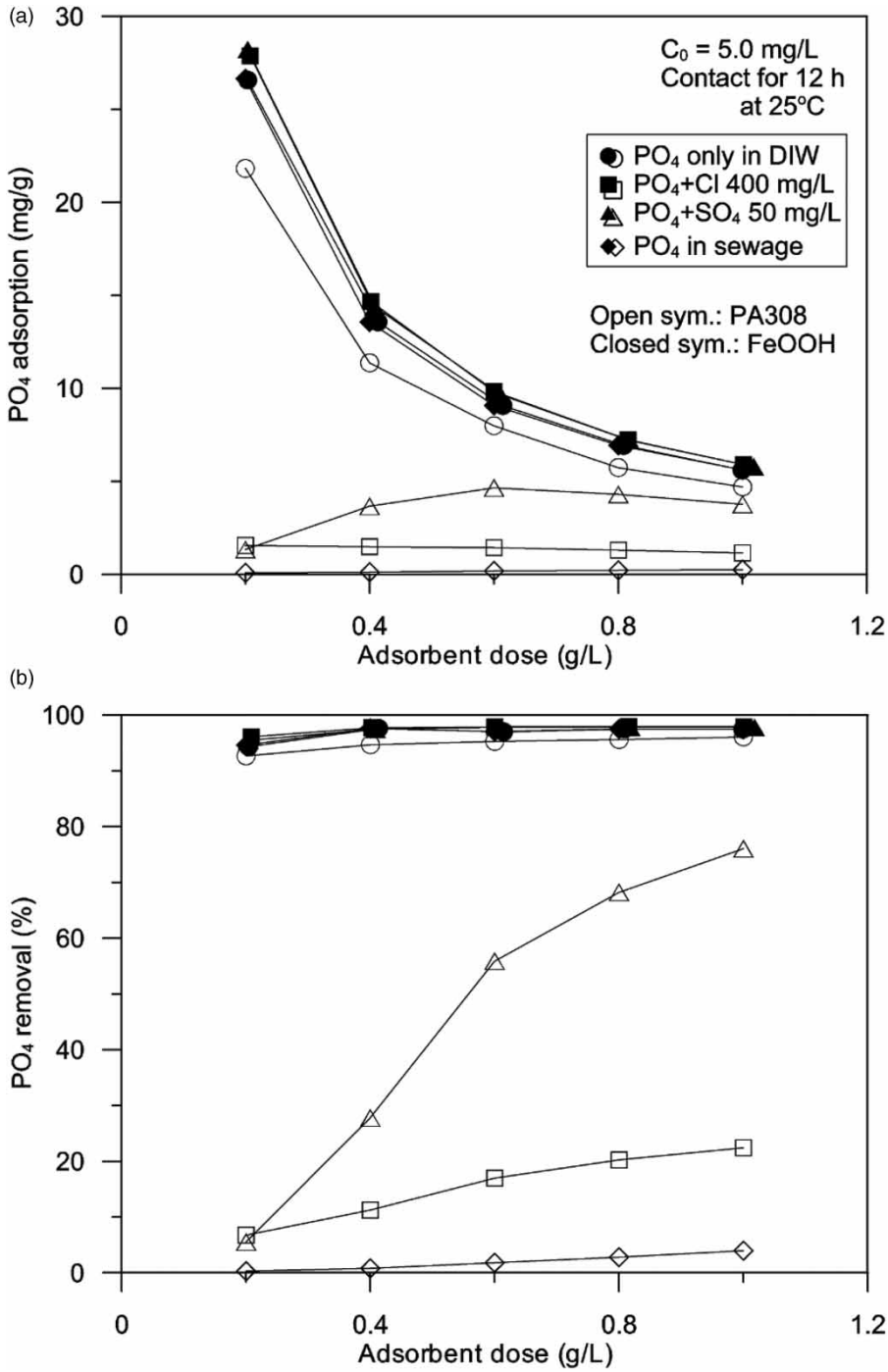

Figure 6 | Effect of co-existing competitive anions on the PO_4-P removal by β-FeOOH and anion-exchange polyamide (PA) resin.

competing anions such as Cl^- and SO_4^{2-} on the uptake of PO_4-P ion onto the β-FeOOH and the commercial polyamide (PA) resin depending on the dose of adsorbent. The experiments were conducted under a binary system, which contains 5 mg/L of PO_4^{3-} ion paired with 400 mg/L of Cl^- ions or 50 mg/L of SO_4^{2-} ion. In which the concentrations of Cl^- and SO_4^{2-} ions are the same values as the concentration of the discharged water used as the real wastewater in this study. As shown in Figure 6, the effects of co-existing competitive anions on PO_4-P adsorption capacity of β-FeOOH were almost negligible in all adsorbent dosage conditions (0.2–1.0 g/L). In contrast, the PA resin showed a significant decrease in adsorption of PO_4-P ions as the presence of competing anions. Furthermore, it is notable that the effects of co-existing anions on PO_4-P adsorption of PA resin were greatly increased as adsorbent doses decreased, because this shows that adsorption competition can take place more intensely under saturation conditions.

To investigate more the interference of co-existing competitive anions, phosphate adsorption was also carried out in the fixed bed column experiments. As shown in Figure 7, the breakthrough curve for phosphate solution ($C_0 = 5$ mg/L as PO_4^{3-} ion) prepared with deionized water for β-FeOOH was similar to the case prepared with the discharge water from sewage treatment plant. Both curves breakthrough at almost the same time although they are slightly different in the shapes that are probably related to the packing properties. Thus it is clear that the ions in the discharge water had a negligible effect on the adsorption of phosphate by β-FeOOH. The adsorption capacities calculated from the ideal breakthrough ($C/C_0 = 0.5$) points were 21.6 mg/g for DIW and 21.3 mg/g for discharge water, which are much lower than that obtained from the batch experiment. This difference is assumed to be caused by the slow adsorption rate of β-FeOOH/PAN bead and the pH difference of the solutions (see Figure 3), although further experiments are needed to determine the exact cause. In contrast, PA resin showed a significant difference in the breakthrough time depending on the blank solution. The results indicated that PA resin hardly adsorbs phosphate from sewage discharge water due to competition with co-existing anions.

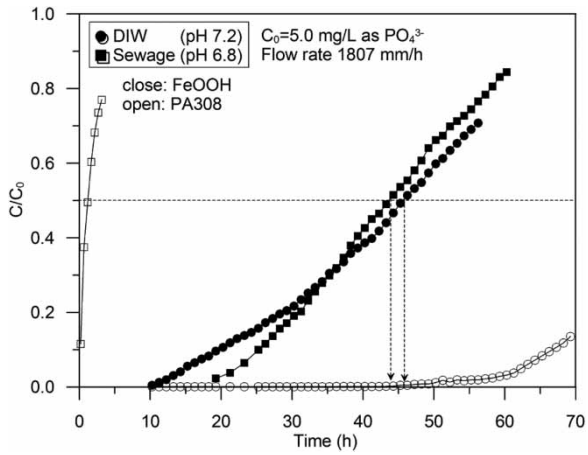

Figure 7 | Breakthrough curves for the removal of PO_4-P by β-FeOOH and polyamide (PA) resin at different chemical composition of base solution.

From these results, it is obvious that β-FeOOH has a high affinity for the PO_4-P anion and there is no significant influence of competing anions on its PO_4-P adsorption capacity, and hence that β-FeOOH can be used effectively as a phosphate-selective adsorbent.

Regeneration efficiency

In order to assess the possibility of recycling the adsorbent for reuse in multiple adsorption cycles, repeated adsorption–regeneration experiments were performed. Phosphate desorption experiments for the used β-FeOOH were conducted using 0.1 M NaOH solution, where the 100 mL fraction of NaOH solution was added per gram of phosphate-loaded β-FeOOH and stirred for 1 h at 25 °C. As shown in Figure 8, the adsorption capacity remained almost constant regardless of the number of regeneration cycles. As a result, β-FeOOH could be regenerated by a simple alkali washing process without lowering the adsorption capacity and thus, could be used more than 10 times maintaining the same adsorbent quality.

CONCLUSIONS

The phosphate adsorption capacity was increased to β-FeOOH > PA resin > $Fe(OH)_3$ and showed high adsorption capacity when the ferric iron was processed in the form of β-FeOOH. The adsorption behavior of β-FeOOH for phosphate anions could be explained by both the Langmuir isotherm model and the Freundlich isotherm model, but it showed a better match for the Langmuir model. The maximum adsorption capacity of β-FeOOH for phosphate was found to be 60.98 mg/g from the Langmuir model. The adsorption process was found to follow a pseudo-second-order kinetic model. The phosphate adsorption capacity of β-FeOOH was high at acidic pH values below 6, but sharply decreased with increase in pH higher than 7. The phosphate adsorption capacity of β-FeOOH was not affected at all by the co-existence of competing anions, such as Cl^- ion or

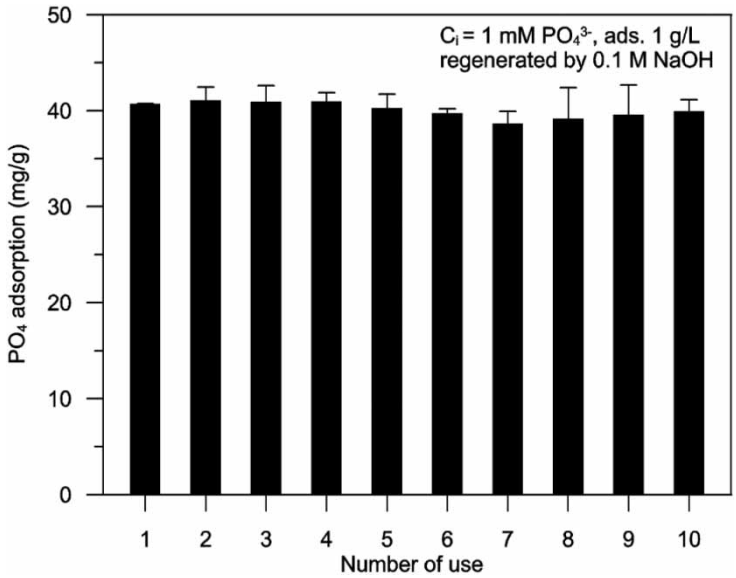

Figure 8 | Regeneration efficiency of β-FeOOH by 0.1 M NaOH washing.

SO_4^{2-} ions contained in large quantities in the sewage. β-FeOOH could be regenerated by a simple washing process using NaOH solution and could be used more than 10 times while retaining the same adsorption capacity. The results of this present investigation suggest that β-FeOOH can be used as a phosphate-selective adsorbent and the adsorption process using β-FeOOH can be efficiently utilized to the phosphate removal systems of sewage treatment plants.

ACKNOWLEDGEMENT

This research was supported by the National Research Foundation of Korea (NRF-2020R1I1A1A01070853).

DATA AVAILABILITY STATEMENT

All relevant data are included in the paper or its Supplementary Information.

REFERENCES

Ajmal, Z., Muhmood, A., Usman, M., Kizito, S., Lu, J., Dong, R. & Wu, S. 2018 Phosphate removal from aqueous solution using iron oxides: adsorption, desorption and regeneration characteristics. *Journal of Colloid and Interface Science* **528**, 145–155.

Bondy, S. C. 2014 Prolonged exposure to low levels of aluminum leads to changes associated with brain aging and neurodegeneration. *Toxicology* **315**, 1–7.

Chitrakar, R., Tezuka, S., Sonoda, A., Sakane, K., Ooi, K. & Hirotsu, T. 2006 Phosphate adsorption on synthetic goethite and akaganeite. *Journal of Colloid and Interface Science* **298**, 602–608.

Conley, D. J., Paerl, H. W., Howarth, R. W., Boesch, D. F., Seitzinger, S. P., Havens, K. E., Lancelot, C. & Likens, G. E. 2009 Controlling eutrophication: nitrogen and phosphorus. *Science* **323**, 1014–1015.

Fan, Y., Li, Y., Wu, D., Li, C. & Kong, H. 2017 Application of zeolite/hydrous zirconia composite as a novel sediment capping material to immobilize phosphorus. *Water Research* **123**, 1–11.

Freundlich, H. M. F. 1906 Over the adsorption in solution. *Journal of Physical Chemistry* **57**, 85–470.

Fu, H., Yang, Y., Zhu, R., Liu, J., Usman, M., Chen, Q. & He, H. 2018 Superior adsorption of phosphate by ferrihydrite-coated and lanthanum decorated magnetite. *Journal of Colloid and Interface Science* **530**, 704–713.

Gajewska, M., Kopeć, Ł. & Obarska-Pempkowiak, H. 2011 Operation of small wastewater treatment facilities in a scattered settlement. *Rocznik Ochrona Środowiska (Annual Set the Environment Protection)* **13**, 207–225.

Genkai-Kato, M. & Carpenter, S. R. 2005 Eutrophication due to phosphorus recycling in relation to lake morphometry, temperature, and macrophytes. *Ecology* **86**, 210–219.

Genz, A., Kornmuler, A. & Jekel, M. 2004 Advanced phosphorus removal from membrane filtrates by adsorption on activated aluminum oxide and granulated ferric hydroxide. *Water Research* **38**, 3523–3530.

Gogate, P. R. & Pandit, A. B. 2004 A review of imperative technologies for wastewater treatment II: hybrid methods. *Advances in Environmental Research* **8**, 553–597.

Ho, Y. & McKay, G. 1998 A comparison of chemisorption kinetic models applied to pollutant removal on various sorbents. *Transactions of the Institution of Chemical Engineers B* **76**, 332–340.

Jiang, J., Kim, D. I., Dorji, P., Phuntsho, S., Hong, S. & Shon, H. K. 2019 Phosphorus removal mechanisms from domestic wastewater by membrane capacitive deionization and system optimization for enhanced phosphate removal. *Process Safety and Environmental Protection* **126**, 44–52.

Kantipuly, C., Katragadda, S., Chow, A. & Gesser, H. 1990 Chelating polymers and related supports for separation and preconcentration of trace metals. *Talanta* **37**, 491–517.

Kasprzyk, M. & Gajewska, M. 2019 Phosphorus removal by application of natural and semi-natural materials for possible recovery according to assumptions of circular economy and closed circuit of P. *Science of the Total Environment* **650**, 249–256.

Kochian, L. V. & Jones, D. L. 1997 Aluminum toxicity and resistance in plants. In: *Research Issues in Aluminum Toxicity* (R. A. Yokel & M. S. Golub eds). Taylor and Francis, Washington, pp. 69–90.

Krom, M. D. & Berner, R. A. 1980 Adsorption of phosphate in anoxic marine sediments 1. *Limnology and Oceanography* **25**, 797–806.

Kurzbaum, E. & Bar Shalom, O. 2016 The potential of phosphate removal from dairy wastewater and municipal wastewater effluents using a lanthanum-modified bentonite. *Applied Clay Science* **123**, 182–186.

Lagergren, S. 1898 About the theory of so-called adsorption of soluble substances. *K. Sven. Ventenskasakad. Handl.* **24**, 1–39.

Langmuir, I. 1918 The adsorption of gases on plane surfaces of glass, mica and platinum. *The Journal of the American Chemical Society* **40**, 1361–1403.

Lewis Jr, W. M., Wurtsbaugh, W. A. & Paerl, H. W. 2011 Rationale for control of anthropogenic nitrogen and phosphorus to reduce eutrophication of inland waters. *Environmental Science & Technology* **45**, 10300–10305.

Li, Y., Fu, F., Cai, W. & Tang, B. 2019 Synergistic effect of mesoporous feroxyhyte nanoparticles and Fe(II) on phosphate immobilization: adsorption and chemical precipitation. *Powder Technology* **345**, 786–795.

Méndez-Álvarez, E., Soto-Otero, R., Hermida-Ameijeiras, Á., López-Real, A. M. & Labandeira-García, J. L. 2002 Effects of aluminum and zinc on the oxidative stress caused by 6-hydroxydopamine autoxidation: relevance for the pathogenesis of Parkinson's disease. *Biochimica et Biophysica Acta (BBA)-Molecular Basis of Disease* **1586**, 155–168.

Omwene, P. I., Kobya, M. & Can, O. T. 2018 Phosphorus removal from domestic wastewater in electrocoagulation reactor using aluminum and iron plate hybrid anodes. *Ecological Engineering* **123**, 65–73.

Park, H. J. & Na, C. K. 2009 Adsorption characteristics of anionic nutrients onto the PP-g-AA-Am non-woven fabric prepared by photoinduced graft and subsequent chemical modification. *Journal of Hazardous Materials* **166**, 1201–1209.

Park, H. J., Nguyen, D. C. & Na, C. K. 2015 Phosphate removal from aqueous solutions using (vinylbenzyl) trimethylammonium chloride grafted onto polyester fibers. *Water Science and Technology* **71**, 1875–1883.

Park, T., Ampunan, V., Lee, S. & Chung, E. 2016 Chemical behavior of different species of phosphorus in coagulation. *Chemosphere* **144**, 2264–2269.

Schindler, D. W., Carpenter, S. R., Chapra, S. C., Hecky, R. E. & Orihel, D. M. 2016 *Reducing Phosphorus to Curb Lake Eutrophication is A Success*. ACS Publications.

Sendrowski, A. & Boyer, T. H. 2013 Phosphate removal from urine using hybrid anion exchange resin. *Desalination* **322**, 104–112.

Villalba, J. C., Constantino, V. R. & Anaissi, F. J. 2010 Iron oxyhydroxide nanostructured in montmorillonite clays: preparation and characterization. *Journal of Colloid and Interface Science* **349**, 49–55.

Wang, Y., Yu, Y., Li, H. & Shen, C. 2016 Comparison study of phosphorus adsorption on different waste solids: fly ash, red mud and ferric–alum water treatment residues. *Journal of Environmental Sciences* **50**, 79–86.

Wu, Y., Li, X., Yang, Q., Wang, D., Xu, Q., Yao, F., Chen, F., Tao, Z. & Huang, X. 2019 Hydrated lanthanum oxide-modified diatomite as highly efficient adsorbent for low-concentration phosphate removal from secondary effluents. *Journal of Environmental Management* **231**, 370–379.

Yan, L., Xu, Y., Yu, H., Xin, X., Wei, Q. & Du, B. 2010 Adsorption of phosphate from aqueous solution by hydroxy-aluminum, hydroxy-iron and hydroxy-iron–aluminum pillared bentonites. *Journal of Hazardous Materials* **179**, 244–250.

Yang, Q., Wang, X., Luo, W., Sun, J., Xu, Q., Chen, F., Zhao, J., Wang, S., Yao, F. & Wang, D. 2018 Effectiveness and mechanisms of phosphate adsorption on iron-modified biochars derived from waste activated sludge. *Bioresource Technology* **247**, 537–544.

Yin, H., Yun, Y., Zhang, Y. & Fan, C. 2011 Phosphate removal from wastewaters by a naturally occurring, calcium-rich sepiolite. *Journal of Hazardous Materials* **198**, 362–369.

Zhang, M., Gao, B., Yao, Y., Xue, Y. & Inyang, M. 2012 Synthesis of porous MgO-biochar nanocomposites for removal of phosphate and nitrate from aqueous solutions. *Chemical Engineering Journal* **210**, 26–32.

Zhang, H., Elskens, M., Chen, G. & Chou, L. 2019 Phosphate adsorption on hydrous ferric oxide (HFO) at different salinities and pHs. *Chemosphere* **225**, 352–359.

Zhao, W., Zhang, Y., Lv, D., Wang, M., Peng, Y. & Li, B. 2016 Advanced nitrogen and phosphorus removal in the pre-denitrification anaerobic/anoxic/aerobic nitrification sequence batch reactor (pre-A2NSBR) treating low carbon/nitrogen (C/N) wastewater. *Chemical Engineering Journal* **302**, 296–304.

First received 31 December 2020; accepted in revised form 21 April 2021. Available online 10 May 2021